Optics Communications 410 (2018) 889–895

Contents lists available at ScienceDirect

Optics Communications

journal homepage: www.elsevier.com/locate/optcom

Multi-LED parallel transmission for long distance underwater VLC system with one SPAD receiver

Chao Wang *, Hong-Yi Yu, Yi-Jun Zhu, Tao Wang, Ya-Wei Ji

National Digital Switching System Engineering & Technological Research Center, Zhengzhou, Henan Province (450000), China

ARTICLE INFO

Keywords:
Underwater visible light communication
Multiple light emitting diode
Single photon avalanche diode
Poisson
Photon-counting
Successive interference cancellation

ABSTRACT

In this paper, a multiple light emitting diode (LED) chips parallel transmission (Multi-LED-PT) scheme for underwater visible light communication system with one photon-counting single photon avalanche diode (SPAD) receiver is proposed. As the lamp always consists of multi-LED chips, the data rate could be improved when we drive these multi-LED chips parallel by using the interleaver-division-multiplexing technique. For each chip, the on–off-keying modulation is used to reduce the influence of clipping. Then a serial successive interference cancellation detection algorithm based on ideal Poisson photon-counting channel by the SPAD is proposed. Finally, compared to the SPAD-based direct current-biased optical orthogonal frequency division multiplexing system, the proposed Multi-LED-PT system could improve the error-rate performance and anti-nonlinearity performance significantly under the effects of absorption, scattering and weak turbulence-induced channel fading together.

1. Introduction

Nowadays, the light emitting diode (LED) devices have been widely used for green lighting and electronic products. As a result, the LED-based visible light communication (VLC) is attracting extensive attention. Meanwhile, the underwater VLC (UVLC) develops rapidly due to potential high data rate, low attenuation and scattering effects in the blue–green light spectrum region [1–7]. However, the effects of absorption, scattering and turbulence in the underwater channel make the practical communication distance of UVLC is limit 100 m even in the pure seawater [1,2,7].

To combat the three damaging effects and realize the long distance transmission, the single photon avalanche diodes (SPAD) devices are used for UVLC because of its high sensitivity. The channel estimation and multiple-symbol detection technologies are studied for the long distance SPAD-based UVLC system with lognormal turbulence model [7]. However, unlike photodiode (PD)-based VLC systems with the additive white Gaussian noise (AWGN) channel [1–3], the conventional AWGN detection theory cannot be directly utilized in the SPAD-based VLC system because of the ideal Poisson photon-counting output distribution of SPAD receiver [8–13].

To improve the data rate by the multi-LED chips in one commercial LED lamp, the superposed pulse amplitude modulation and phase-shifted superposition modulation have been proposed for indoor VLC systems [14,15]. Based on driving multi-LED chips in parallel, the bandwidth efficiency can be improved and the multiplexing gains can be achieved even though the on–off keying (OOK) modulation is applied. In fact, the signals from the parallel multi-LED chips are equivalent to be a high order signal constellation. As a result, compared to the OOK scheme, the direct current (DC)-biased optical orthogonal frequency division multiplexing (DCO-OFDM) is susceptible from the LED nonlinear effect with the high peak-to-average power ratio (PAPR) [8].

However, at present, there are no corresponding research about the long distance turbulence-based UVLC system with the multi-LED chips parallel high speed transmission method. Hence, in this paper, we propose a multi-LED chips parallel transmission (Multi-LED-PT) scheme with one SPAD receiver for the long distance UVLC system by combining the effects of absorption, scattering and weak turbulence together. To distinguish the superposed photon-counting signals by different LED chips, the user-specific interleavers with interleaver-division-multiplexing technique are used for increasing the degree of freedom for signal detection [16,17]. In addition, a serial successive interference cancellation (SIC) detection algorithm based on ideal Poisson photon-counting channel by the SPAD receiver is proposed. Finally, the simulation results show that our proposed Multi-LED-PT scheme outperforms that of the SPAD-based DCO-OFDM scheme in terms of error-rate performance and anti-nonlinearity performance.

* Corresponding author.
E-mail addresses: xxgcwangchao@163.com (C. Wang), maxyucn@163.com (H.-Y. Yu), yijunzhu1976@outlook.com (Y.-J. Zhu), yjswangtao@163.com (T. Wang), jiyw1103@foxmail.com (Y.-W. Ji).

https://doi.org/10.1016/j.optcom.2017.11.069
Received 3 October 2017; Received in revised form 7 November 2017; Accepted 24 November 2017
Available online 14 December 2017
0030-4018/

Fig. 1. The multi-LED chips in one commercial LED lamp.

2. System model

The structure of the proposed long distance SPAD-based Multi-LED-PT photon-counting system is shown in Fig. 2. The intensity modulation with direct detection (IM/DD) technique are generally used in VLC system. As a result, the channel coefficients and the transmitted signals by the LED devices are nonnegative. Furthermore, the average optical power is given by the average signal amplitude, rather than the average square amplitude as the radio frequency communication, i.e.

$$s(t) \geq 0, \quad h(t) \geq 0, \quad P_t = \lim_{x\to 0} \frac{1}{2x} \int_{-x}^{x} s(t)dt, \tag{1}$$

where $s(t)$ is the transmitted signal, $h(t)$ denotes the channel and P_t is the average optical power.

2.1. The transmitter of multi-LED chips

The binary bit sequence $\mathbf{u}$ is divided into K data streams after serial-to-parallel (S/P) conversion, where K is the number of LED chips in one lamp. Then the data bits $\mathbf{u}_k = \{u_k(1), u_k(2), \ldots, u_k(l_b)\}$ are coded by a binary encoder (Enc) which generate a coded sequence $\mathbf{c}_k = \{c_k(1), c_k(2), \ldots, u_k(J)\}$, where l_b is the data frame length of each LED chip and J is the total frame length. $\mathbf{v}_k = \{v_k(1), v_k(2), \ldots, v_k(J)\}$ are the data when the $\mathbf{c}_k$ are permutated by a user-specific interleaver-k (Π_k) proposed in [16,17]. s_k is the output data after the Non-Return-to-Zero OOK modulation. Finally, the signals from different LED chips are mixed when the light beam passes through the lampshade.

The exclusive differences among different LED wicks are the different interleavers. The pivotal principle of this scheme is that the interleavers should be orthogonal for different LED wicks. In other words, the adjacent signals after the processing of interleave are approximately uncorrelated. By using the user-specific interleaver of each LED wick [16,17], the superposed signals can be detected at the receiver. Therefore, all the transmitters can be independent to achieve multiple times spectral efficiency for increasing the data rate.

2.2. UVLC channel model for multi-LED chips

The diffusion length can be considered as the longest distance that a photon could travel theoretically, which is defined as $\tau = c_w L$, where c_w denotes the cumulative attenuation coefficient and L is the communication distance. According to the contributions of UVLC channel model in [2,7,11], the underwater channel can be regarded as non-dispersive when the data rate is $R_b < 50$ Mbps and the diffusion length is $\tau < 15$ for the pure seawater or clear ocean condition. Hence, the inter-symbol interference could be neglected in the following analysis.

As the UVLC channel model in [6,7], the accumulated UVLC channel impulse response between the transmitter and the receiver is $h = h_t h_{cw}$ [6,7], where h_{cw} is the fading-free impulse response due to the absorption and scattering effects, and h_t denotes the randomly weak oceanic fluctuations fading. In addition, h_t is modeled as a lognormal fading model

$$f(h_t) = \frac{1}{2h_t\sqrt{2\pi\sigma^2}} \exp\left(-\frac{(\ln h_t - 2\mu)^2}{8\sigma^2}\right), \tag{2}$$

where σ^2 is the variance and μ is the mean of the weak ocean turbulence channel h_t. The fading amplitude is normalized as $E[h_t] = 1$ to ensure that fading neither attenuates nor amplifies the average power, i.e. $\mu = -\sigma^2$.

The distance from the LED lamp to the SPAD is more than 50 m [7,11], while the distance among different LED chips in one lamp is only several centimeters as Fig. 1. Therefore, we assume that the channel impulse responses from different LED chips to the receiver are equal. Without loss of generality, the channel gain $\mathbf{h}$ can be given by

$$\mathbf{h} = [h(1), h(2), \ldots, h(K)] = h[1, 1, \ldots, 1]. \tag{3}$$

Meanwhile, h can be regarded as a constant over a relatively short time period.

2.3. The photon-counting model of SPAD receiver

The received photon counts before SPAD in one bit period time can be calculated by

$$r(j) = c_p n_s \mathbf{h}\mathbf{s}(j) + c_p n_b + N_d T_b = c_p n_s \mathbf{h}\mathbf{s}(j) + n(j), \tag{4}$$

where c_p is the photon detection efficiency (PDE). The transmitted photons of each LED chip is $n_s = P_s T_b / E_p K$, where P_s is the total optical power of the LED, T_b is the bit duration and $R_b = 1/T_b$ is the given bit data rate. $E_p = h_p \nu/\lambda$ is the energy of one photon, where h_p is the Planck' constant, ν is the light speed in the water. $\mathbf{s}(j) = [s_1(j), s_2(j), \cdots, s_K(j)]^T$ is a $K\times 1$ transmitted signal vector whose entries are chosen randomly, equally-likely, independently distribution from an OOK modulation constellation. The power of LED is $2P_s$ and 0 when bit "1" and bit "0" are transmitted respectively. $n_b = P_b T_b / E_p$ is the photons caused by the background noise, N_d is the dark count ratio (DCR) of SPAD, and $n(j)$ is the sum photon value of background

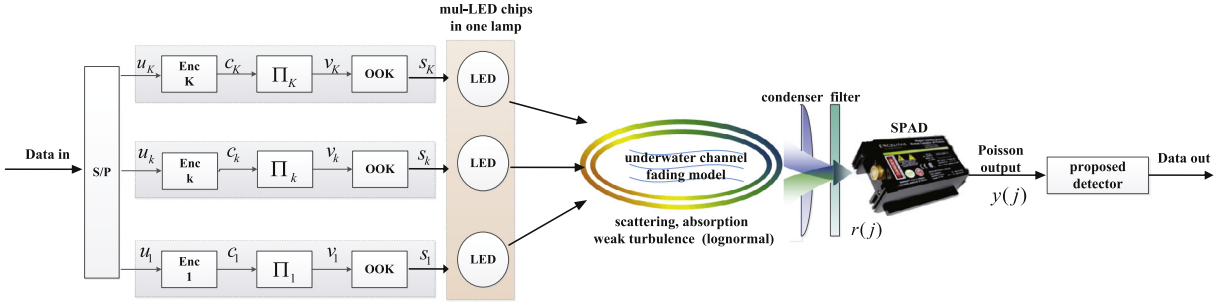

Fig. 2. The system model of the proposed UVLC scheme.

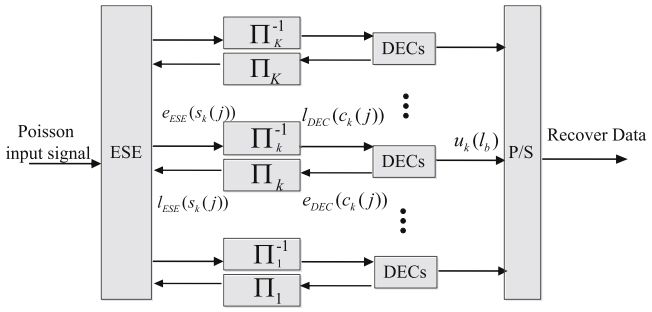

Fig. 3. The proposed model of receiver.

light and dark count. The ideal output of SPAD could be modeled as ideal Poisson statistics distribution [7–11] with the probability mass function (PMF)

$$Pr(y(j)|\mathbf{s}(j),\mathbf{h}) = \frac{r(j)^{y(j)}}{y(j)!}\exp^{-r(j)}. \tag{5}$$

3. The detection algorithm

In this section, a serial SIC iterative detection receiver based on Poisson channel is presented to detect the received mixed photon-counting signals. The proposed receiver includes an elementary signal estimator (ESE) and K soft input soft output decoders (DECs) as Fig. 3. The ESE gives an estimation of the transmitted signal of each LED chip, which is then sent to the DECs to generate extrinsic information. The information is fed back to the ESE in the next iteration to improve the accuracy. It is assumed that the receiver executes the ESE of chip-1 firstly and treats all non-chip-1 signals as an equivalent noise components. The soft information generated by the ESE is transmitted to the DECs as the priori information after deinterleaving Π_1^{-1}. Then the DECs generates soft information by a standard posteriori probability (APP) algorithm and updates the total soft information of the ESE after interleaving Π_1. This process continues iteratively for a preset number of iterations. Finally, the hard decision is used to restore the original data after the parallel-to-serial (P/S) conversion.

3.1. The ESE part

For the OOK modulation used in this paper, we define the priori log likelihood ratios (LLRs) of ESE and DECs respectively as

$$l_{ESE}(s_k(j)) = \log\frac{Pr(s_k(j)=1)}{Pr(s_k(j)=0)}, \tag{6}$$

$$l_{DECs}(c_k(j)) = \log\frac{Pr(c_k(j)=1)}{Pr(c_k(j)=0)}, \tag{7}$$

where $l_{ESE}(s_k(j))$ is applied in ESE as the input soft information of chip-k and $l_{DECs}(c_k(j))$ is the input of decoder. To calculate the soft information of chip-k, we define the non chip-k information as an equivalent noise $\zeta_k(j)$ which is imposed by the multi-LED chips interference, background noise and the DCR together,

$$\zeta_k(j) = c_p n_s h\sum_{\hat{k}\neq k}^{K} s_{\hat{k}}(j) + n_{\hat{k}}(j). \tag{8}$$

Hence, according to (5), the PMF of the receiver for the k_{th} chip is given by

$$\begin{aligned} &Pr(y(j)|s_k(j),\mathbf{h}) \\ &= \frac{(c_p n_s h s_k(j)+\zeta_k(j))^{y(j)}}{y(j)!}\exp^{-(c_p n_s h s_k(j)+\zeta_k(j))}. \end{aligned} \tag{9}$$

Finally, for the Poisson output of SPAD, the extrinsic LLRs of $e_{ESE}(x_k(j))$ is calculated as

$$\begin{aligned} e_{ESE}(x_k(j)) &= \log\frac{Pr(y(j)|s_k(j)=1,\mathbf{h})}{Pr(y(j)|s_k(j)=0,\mathbf{h})} \\ &= \log\frac{\frac{(c_p n_s h+\zeta_k(j))^{y(j)}}{y(j)!}\exp^{-(c_p n_s h+\zeta_k(j))}}{\frac{\zeta_k(j)^{y(j)}}{y(j)!}\exp^{-\zeta_k(j)}} \\ &= y(j)\log(1+\frac{c_p n_s h}{\zeta_k(j)}) - c_p n_s h. \end{aligned} \tag{10}$$

3.2. The noise estimate part

For the characteristic of Poisson distribution, the exclusive impact factor is the mean value λ. Hence the mean value of $\zeta_k(j)$ can be estimated as

$$E[\zeta_k(j)] = c_p n_s h\sum_{\hat{k}\neq k}^{K} E[s_{\hat{k}}(j)] + n_{\hat{k}}(j), \tag{11}$$

where the mean value of $s_k(j)$ is

$$\begin{aligned} E[s_k(j)] &= 1\times Pr(s_k(j)=1) + 0\times Pr(s_k(j)=0) \\ &= 0.5\times\tanh(l_{ESE}(s_k(j))/2) + 0.5. \end{aligned} \tag{12}$$

The initialized value is $E[s_k(j)] = 0.5\times 1 + 0.5\times 0 = 0.5$, as there is no priori information in the ESE module initially.

3.3. The matched repetition code structure for OOK

In an IM/DD system, the transmitted signal and channel coefficient are nonnegative. Consequently, the repetition code is $\mathbf{c} = \{1,1,\ldots,1\}_m$, where m is the code length. In other words, the function of the repetition code is to map the information bit for a length of m, e.g. bit "0"$\Rightarrow \{0,0,\ldots,0\}_m$, or "1"$\Rightarrow \{1,1,\ldots,1\}_m$. Finally, the decoded LLRs $l(u_k(l_b))$ can be given by

$$\begin{aligned} l(u_k(l_b)) &= \log\frac{Pr(u_k(l_b)=1)}{Pr(u_k(l_b)=0)} = \log\frac{\prod_{j=1}^{m} Pr(c_k(j)=1)}{\prod_{j=1}^{m} Pr(c_k(j)=0)} \\ &= \sum_{j=1}^{m}\log\frac{Pr(c_k(j)=1)}{Pr(c_k(j)=0)} = \sum_{j=1}^{m} l_{DECs}(c_k(j)). \end{aligned} \tag{13}$$

Therefore, the $e_{DECs}(c_k(j))$ is calculated as

$$\begin{aligned} e_{DECs}(c_k(j)) &= \log\frac{Pr(c_k(j)=1|l(u_k(l_b)))}{Pr(c_k(j)=0|l(u_k(l_b)))} - l_{DEC}(c_k(j)) \\ &= n_k(j) l(u_k(l_b)) - l_{DEC}(c_k(j)) \\ &= l(u_k(l_b)) - l_{DEC}(c_k(j)). \end{aligned} \tag{14}$$

3.4. The DECs part

After the last iteration, the symbol judgment $\hat{u_k}(l_b)$ which follows the APP hard decision rule is deduced as

$$\hat{u_k}(l_b) = \begin{cases} 1, l(u_k(l_b)) \geq 0; \\ 0, l(u_k(l_b)) < 0. \end{cases} \tag{15}$$

3.5. The complexity

The above procedures are the main signal processing steps of the receiver. The operations of one iteration are composed of several multiplications, several additions and a tanh computation. The main complexity of the system comes from the process of interleaving and deinterleaving. Finally, we summarize the above detection procedures in Algorithm 1.

Table 1
Detailed parameters of our proposed system.

Water type	Absorption	Scattering	Cumulative attenuation	Communication diastance	τ	Data rate of single LED chip
Pure seawater	0.053 1/m	0.003 1/m	0.056 1/m	220 m	12.32	1, 10, 50 Mbps
Clean ocean	0.069 1/m	0.08 1/m	0.15 1/m	100 m	15	1, 10, 50 Mbps

Table 2
Parameters for the SPAD device.

Wavelength of light (w)	532 nm
The PDE of the SPAD (c_p)	0.5
The DCR of the SPAD (N_d)	50 count/s
The half power angle of LED	5°
The light speed in the water	2.25×10^8 m/s
Typical maximum count rate	40 Mc/s
Timing resolution	350 ps

Algorithm 1: Multi-LED-PT for UVLC system.

Step 1. SIC detection based on Poisson receiver
(1) Initialization: For the OOK modulation, $E[s_k(j)]=0.5$ and $e_{ESE}(x_k(j))=0$;
(2) Execute the noise estimate part, and calculate $E[\zeta_k(j)]$ by (11);
(3) Execute the ESE part, and calculate the extrinsic LLRs $e_{ESE}(x_k(j))$ by (10);
(4) The repetition code gains $l(u_k(l_b))$ can be obtained by (13) after the deinterleaving, which could be used for decoding;
(5) Produce the extrinsic LLRs $e_{DECs}(c_k(j))$ by (14);
(6) Update the noise estimate part by (12) after the interleaving;
(7) For a new iteration procedure, we execute the (1) of Step 1 for a new circulation.

Step 2. Symbol judgment
After the final iteration, the APP hard decoding rule is used for symbol judgment as in (15). Finally, we could recover the data signals **u** by the P/S conversion.

4. Computer simulation results

In the section, we consider an SPAD-based Multi-LED-PT photon-counting UVLC system by combining the effects of absorption, scattering and weak turbulence together, then we carry out some computer simulations to verify our analysis.

The simulations of absorption and scattering are based on the large scale Monte Carlo Numerical Simulation (MCNS) as [11]. Meanwhile, the weak turbulence-induced channel fading is based on the analysis as [7].

As the parameters used in [7,11], the fading-free impulse response h_c is 10^{-8} which corresponds to the communication distances L are 100 and 220 m for clear ocean and pure seawater respectively [7,11]. Usually, the background noise P_b comes from the sunlight, hence we assume that the $P_b=-116$ dBm under the water depth of nearly 150 m [2,7]. The number of iterations is 5 unless we analyze the convergence problem of the SIC detection algorithm.

In this work, because we narrow the polar angle of LED and improve the power intensity, the underwater channel could be regarded as non-dispersive when the water qualities (the diffusion length $\tau < 15$) are relatively good and the data rates are below than 50 Mbps. The detailed parameters of our proposed system are listed in Table 1. Finally, the other detailed parameters about the SPAD are given in Table 2.

4.1. The feasibility of the proposed system under one LED chip

To verify the system feasibility, we compare the proposed SIC algorithm with the maximum likelihood (ML) algorithm under one LED chip. The code rate is $R_{ca}=1$, which means no channel code.

For an OOK constellation, when the priori probability is $P(s(k)=1)=P(s(k)=0)=0.5$, the ML rule can be presented as: the optimum detection threshold ρ is the intersection point of curve $Pr(\rho|s(k)=1,\mathbf{h})$ and $Pr(\rho|s(k)=0,\mathbf{h})$.

$$\frac{r(s(k)=1)^{\rho}}{\rho!}e^{-r(s(k)=1)}=\frac{r(s(k)=0)^{\rho}}{\rho!}e^{-r(s(k)=0)}, \tag{16}$$

where the detection threshold is $\rho=\lfloor\frac{r(s(k)=1)-r(s(k)=0)}{\ln(r(s(k)=1)/r(s(k)=0))}\rfloor$ and $\lfloor\rfloor$ denotes the largest positive number lower than ρ.

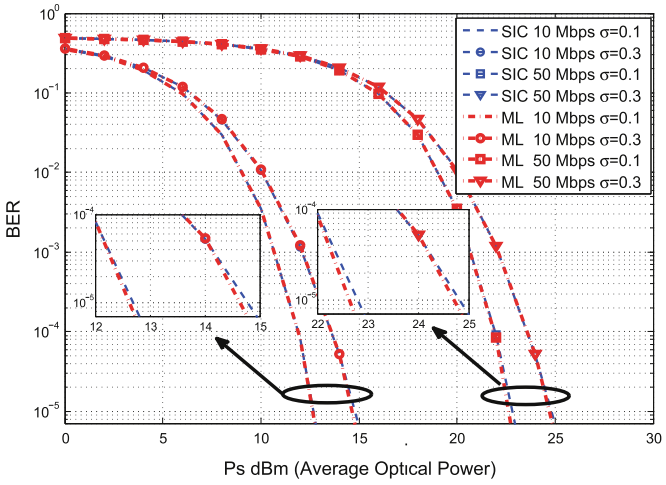

Fig. 4. The different conditions of the proposed system.

From Fig. 4, the SIC algorithm and ML algorithm hold the similar BER under different conditions. Meantime, the BER under 10 Mbps is far better than the 50 Mbps ones. Moreover, the power of the former is less nearly 10 dBm than the latter one when the BER is equal.

When the code rate R_{ca} is lower than 1, i.e. $(1/2, 1/4)$, it is interesting that the proposed system is a specific bit-interleaver-code-modulation/iteration detection (BICM/ID) system [18]. The function of user-specific interleaver would just disorganize the data after channel coding.

4.2. The comparison with SPAD-based DCO-OFDM system

In the following analysis, the multi-LED chips in one lamp work as a parallel form under the proposed scheme and as a serial form under the DCO-OFDM scheme. The high-speed transmission capability and the anti-nonlinearity performance of the SPAD-based Multi-LED-PT system are verified by simulation comparisons with the SPAD-based DCO-OFDM system proposed in [8].

The LED (Seoul Semiconductor F50360) is considered as the light source. The voltage-to-current (V–I) conversion characteristics of the LED is shown in Fig. 5. For the SPAD-based Multi-LED-PT system, each LED chip is biased at the value $V_{DC,i}=2.2$ V, and the linear operating range is 1.8~2.6 V. While for the SPAD-based DCO-OFDM system [8], the DC-bias value is $V_{DC}=2.2\times K$ V; thus, the linear operating range is $1.8\times K\sim 2.6\times K$ V. Therefore, the DC part and illuminating brightness for the two systems are the same.

For the SPAD-based DCO-OFDM system, the subcarriers number is $N_F=1024$ while there are only $N_F/2-1$ independent complex values because of the restriction of IM/DD. The number of guard interval subcarriers is $N_g=4$. The type of subcarrier modulation is quadrature

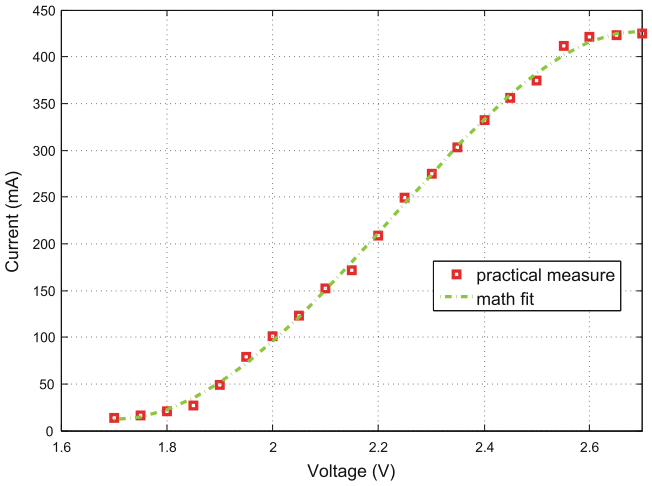

Fig. 5. The V–I characteristics: red dot denotes the measure data, green solid line denotes the math fitting curve. (For interpretation of the references to color in this figure legend, the reader is referred to the web version of this article.)

amplitude modulation (QAM). Hence, the simulation data rate is

$$R_{b,DCO-OFDM} \approx R_s \frac{N_F/2-1}{N_F+N_g}\log_2(D_{QAM}) \approx \frac{1}{2}R_b\log_2(D_{QAM})(\text{Mbps}), \tag{17}$$

where D_{QAM} is the order of QAM.

For the SPAD-based Multi-LED-PT system, the transmitted data of K LED chips are parallel. But the channel repetition code rate R_{ca} of each LED chip will add the code redundancy information. To ensure the pure data rate of the two scheme equivalently, the simulation transmission rate of this system is

$$R_{b,Multi-LED-PT} \approx \frac{R_b \times K}{R_{ca}}(\text{Mbps}). \tag{18}$$

For the purpose of fairness as far as possible, the average optical powers of both systems are equal and the pure data rates of both systems are same. The optical power of each LED chip is P_s/K and the repetition code rate is $R_{ca} = 1/8$. The number of LED chips K are 2, 3, 4, 5 which means the modulation orders D_{QAM} of the DCO-OFDM system are 16, 64, 256, 1024, respectively.

However, for a practical SPAD detector (Excelitas Technologies, SPCM-AQRH-15-FC), the effect of dead time limits the maximum achievable count rates. As a result, the maximum count rate of the commercial SPAD is restricted to a few Mbps [7–9,11]. Hence, to have a comprehensive comparison, we set $R_b = 1$ Mbps and $R_b = 10$ Mbps respectively.

From Figs. 6 and 7, we can obtain the following conclusions:

(1) In the low P_s region, the BER of photon-counting DCO-OFDM system is slightly better than photon-counting Multi-LED-PT scheme.
(2) When the P_s increases, the Multi-LED-PT system requires lower power than DCO-OFDM system to reach the same BER. The reasons are that the signal exceeds the linear dynamic range of the LED chip and the PAPR of the DCO-OFDM increases. As a result, the BER gaps between the Multi-LED-PT and DCO-OFDM schemes become larger when the signal power increases.
(3) When the data rate R_b increases, the BER of DCO-OFDM system with high order QAM constellation could not be below 10^{-3} even though how high the transmitted power is, which denotes the clipping-amplitude noise plays the dominant role. Therefore, compare with the DCO-OFDM system, a better error performance of Multi-LED-PT system in overcoming the nonlinearity of LED is verified.

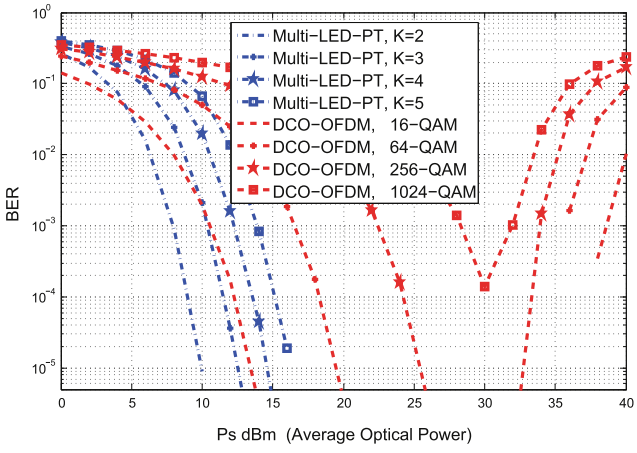

(a) $\sigma = 0.1$.

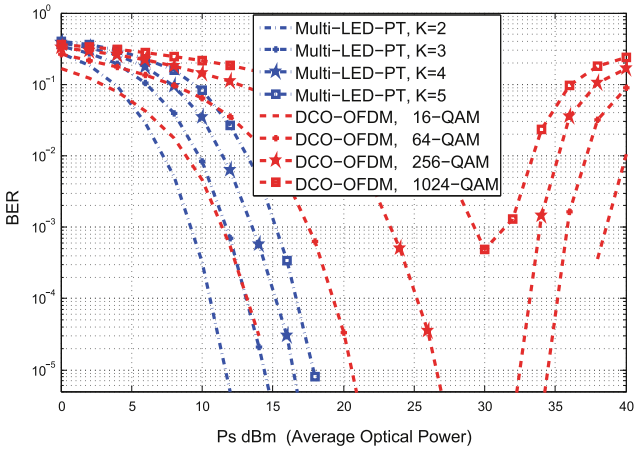

(b) $\sigma = 0.3$.

Fig. 6. BER performance comparison under $R_b = 1$ Mbps.

The above results of our proposed SPAD-based Multi-LED-PT system correspond to the conclusions of the previous indoor PD-based Multi-LED-PT system in [15].

4.3. The rapid convergence under different iterations

The convergence problem of the proposed system could be formulated by estimating the mean value of the LLRs $l(u_k(l_b))$. The converged condition is that $l(u_k(l_b))$ tends to be a constant value after a number of iterations. Then we give some computer simulations to verify the above analysis. The number of LED chips are 1, 2, 4, 8 with $\sigma = 0.2$ and $R_{ca} = 1/8$.

Fig. 8 shows that the proposed system is capable of rapid convergence in underwater weak turbulence lognormal fading channel, and the mean value of the LLRs will be converged after 5 iterations to be a relatively fixed value.

Finally, for an SPAD detector, the system performance will become worse with increasing of the background noise photons. However, an well-designated optical receiver system could be filtered the noise photons as much as possible. The exact analysis of the noise photons is out of the scope of this paper.

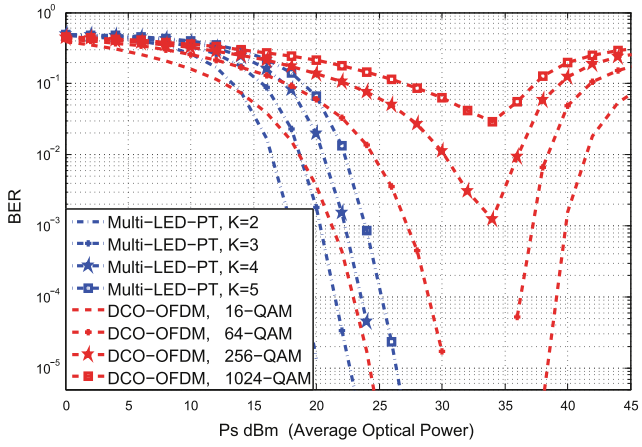

(a) $\sigma = 0.1$.

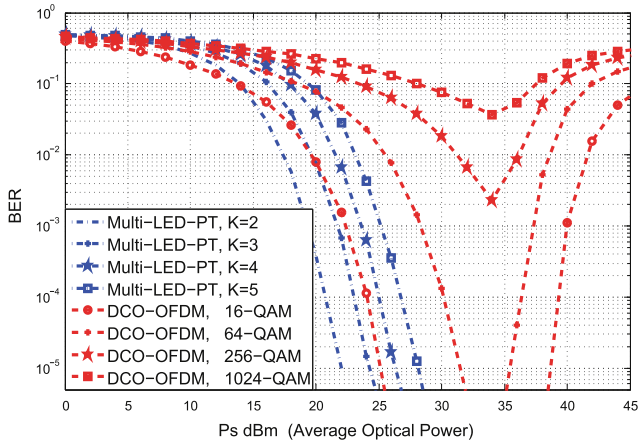

(b) $\sigma = 0.3$.

Fig. 7. BER performance comparison under $R_b = 10$ Mbps.

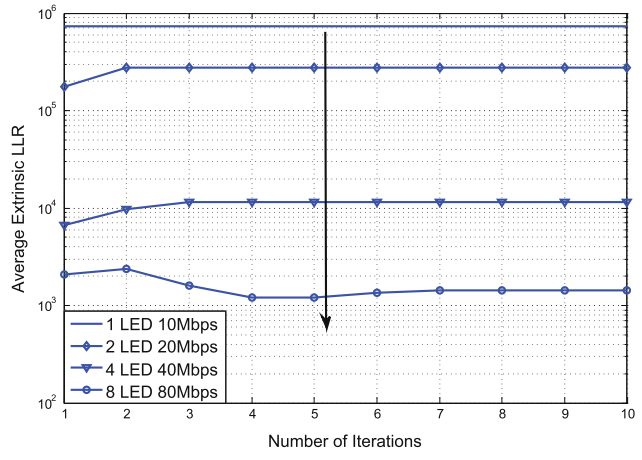

Fig. 8. The rapid convergence under different conditions.

5. Conclusions

In this paper, to increase the data rate of the UVLC system under the absorption, scattering and weak turbulence conditions together, we proposed a Multi-LED-PT photon-counting system with one SPAD receiver. For the ideal Poisson photon-counting output of SPAD, a SIC iteration detection algorithm based OOK constellation was presented. The simulation results showed that the proposed scheme was capable of achieving error resilient and anti-nonlinearity performance with the aid of our flexible multi-LED chips architecture. In fact, the proposed system could be applied in a relay topology network between the users and destinations to increase the communication range and data rate.

In the near future, we will perform some practical experimental measurements on the proposed long distance UVLC Multi-LED-PT system as Fig. 9.

Fig. 9. The water tank used in the practical experiment.

Acknowledgments

This research was sponsored in part by Grant No. 61671477 from China NSFC, and in part by Grant No. 2015B010112001 from Major Scientific and Technological Project of Guangdong Province, China.

References

[1] Z.Q. Zeng, S. Fu, H.H. Zhang, et al., A survey of underwater optical wireless communications, IEEE Commun. Surv. Tutor. 19 (1) (2016) 204–238.
[2] F. Akhoundi, J.A. Salehi, A. Tashakori, Cellular underwater wireless optical CDMA network: Performance analysis and implementation concepts, IEEE Trans. Commun. 63 (3) (2015) 882–891.
[3] S.J. Tang, Y.H. Dong, X.D. Zhang, Impulse response modeling for underwater wireless optical communication links, IEEE Trans. Commun. 62 (1) (2014) 226–234.
[4] H. Gerc, glu. ekcio, Bit error rate of focused Gaussian beams in weak oceanic turbulence, J. Opt. Soc. Amer. A 31 (9) (2014) 1963–1968.
[5] X. Yi, Z. Li, Z. Liu, Underwater optical communication performance for laser beam propagation through weak oceanic turbulence, Appl. Opt. 54 (6) (2015) 1273–1278.
[6] M.V. Jamali, F. Akhoundi, J.A. Salehi, Performance characterization of relay-assisted wireless optical CDMA networks in turbulent underwater channel, IEEE Trans. Wirel. Commun. 15 (6) (2015) 4104–4116.
[7] C. Wang, H.Y. Yu, Y.J. Zhu, et al., Blind detection for SPAD-based underwater VLC system under Poisson-Gaussian mixed noise model, IEEE Commun. Lett. PP (99) (2017) 1–4.
[8] Y.C. Li, M. Safari, R. Henderson, et al., Optical OFDM with Single photon avalanche diode, IEEE Photonics Technol. Lett. 27 (9) (2015) 943–946.
[9] D. Chitnis, S. Collins, A SPAD-based photon detecting system for optical communications, J. Lightwave Technol. 32 (10) (2014) 2028–2034.
[10] T.Q. Mao, Z.C. Wang, Q. Wang, Receiver design for SPAD-based VLC systems under Poisson-Gaussian mixed noise model, Opt. Express 25 (2) (2017) 799.
[11] C. Wang, H.Y. Yu, Y.J. Zhu, Along distance underwater visible light communication system with single photon avalanche diode, IEEE Photonics J. 8 (5) (2016) 7906311.
[12] T. Shafique, O. Amin, M. Abdallah, et al., Performance analysis of single-photon avalanche diode underwater VLC system Using ARQ, IEEE Photonics J. 9 (5) (2017) 2743007.

[13] C. Wang, H.Y. Yu, Y.J. Zhu, et al., Experimental study on SPAD-based VLC systems with an LED status indicator, Opt. Express 25 (23) (2017) 28783–28793.
[14] J.F. Li, Z.T. Huang, R.Q. Zhang, et al., Superposed pulse amplitude modulation for visible light communication, Opt. Express 21 (25) (2013) 31006–31011.
[15] D.F. Zhang, Y.J. Zhu, Y.Y. Zhang, Multi-LED phase-shifted OOK modulation based visible light communication systems, IEEE Photonics Technol. Lett. 25 (23) (2013) 2251–2254.
[16] R. Zhang, L. Hanzo, Space–time coding for high-throughput interleave division multiplexing aided multisource cooperation, Electron. Lett. 44 (5) (2008) 367–368.
[17] P. Li, L.H. Liu, K.Y. Wu, et al., Interleave-division multiple-access, IEEE Trans. Wirel. Commun. 5 (4) (2006) 938–947.
[18] G. Caire, G. Taricco, E. Biglieri, Bit-interleaved coded modulation, IEEE Trans. Inf. Theory 44 (3) (1998) 927–946.